An Alternative Symmetry for Large-Scale Structures in Channel Flow

Tomoaki ITANO*, Sadayoshi TOH** and Kai SATOH***

* Department of Pure and Applied Physics, Faculty of Engineering Science, Kansai University, Suita, Osaka
** Department of Physics and Astronomy, Graduate School of Science, Kyoto University, Kyoto
*** Japan Patent Office, Tokyo

Applying bifurcation analysis in conjunction with direct numerical simulation, two distinct nontrivial equilibrium states in plane Poiseuille flow are obtained. The two states are distinguished by the symmetries imposed. One of these states is of the same form as the exact coherent structure obtained previously by Waleffe. The other state has a pair of counter-rotating streamwise vortices that can develop across the channel midplane, and may provide an exact expression for large-scale structures observed in fully turbulent flow. A truncated dynamical model describing these states predicts that streaky components induced by large-scale circulations spanning the whole of the channel width may survive even in the limit of infinite Reynolds number.

1 INTRODUCTION

Despite the significant progress made since Reynolds' classic experimental observations of 1883, understanding of turbulence remains incomplete, and continues to be a key area of research activity in physics. In the limit as the Reynolds number tends to infinity, turbulent channel flow may be considered to be a multiple system consisting of weakly coupled dynamical systems with hierarchical scales.

At the bottom of the hierarchy, the smallest scale turbulent fluctuations are produced by a number of coherent structures cultivated in the thin high-shear layer near the boundary. Low-speed streaks and streamwise vortices[1,2] are considered to be the representative structures in this layer, and can be educed[3,4] as an equilibrium state by manipulating a balance. For the case of plane Couette flow (PCF), with increasing Reynolds number this state is likely to bifurcate in a self-sustaining cyclic process (SSP)[5,6] embedded in turbulence. It has recently been further suggested that the equilibrium state also constitutes the basin[7] of the turbulent attractor. The resulting theoretical estimation of the threshold of perturbation necessary for turbulent transition is indispensable to state-of-the-art turbulence control techniques[8] . Applying the numerical method proposed[3] into pipe flow, Wedin and Kerswell[9] obtained traveling wave solutions (TWSs), one of which emerges via a saddle-node bifurcation at a value of the Reynolds number that finds good agreement with the experimentally observed critical Reynolds number for turbulent transition.

A fully-developed turbulent state in a channel is not achieved until the coherent structures at the top of the hierarchy propagate fluctuations across the whole of the channel. The resultant universal law of the wall is established subject to scaling laws of the hierarchy from the near-wall to the top (i.e. largest-scale) structures (LSSs). In seeking to better understand turbulence in channel flows, it is thus important to identify the LSSs. One promising candidate to describe the LSSs is the structure composed of streamwise vortical circulations accompanied by low-speed streaky regions of the outer scale (i.e. of the order of the width of the channel), which has recently been attracting a great deal of research attention[10–12] . The LSSs may be self-sustained by some mechanism, or otherwise may be induced by a merging behavior of near-wall structures owing to spanwise modulation[13] or by a cluster of ejection events accompanied with the passage of a streamwise-aligned packets of hairpin vortices[14] . Although such scenarios have been proposed for the formation process of LSSs, there is still insufficient consensus on what precisely defines the nature of these structures.

In the present study, considering possible symmetries for the TWS of plane Poiseuille flow (PPF), we will present exact expressions for LSSs spanning the whole of the channel width. It will be shown that such structures originate at a Reynolds number relatively lower than expected, which may be the starting point at which the scale separation in turbulent flow begins. Furthermore, based on a truncated dynamical model, we predicts that asymptotic structures of the present solutions survive in the limit of infinite Reynolds number. This suggests the present solutions may be relevant to the description of LSSs observed in fully turbulent channel flow.

2 NUMERICAL METHOD

First suppose a channel between infinite parallel plates (walls) filled with incompressible Newtonian fluid, which is driven by a constant pressure gradient imposed in the downstream direction. A Cartesian coordinate system is introduced with the x, y and z axes in the streamwise, wall-normal and spanwise directions, respectively, and the origin located on the channel mid-plane. Based on a non-dimensionalization employing half the channel width (h), a representative velocity and the kinematic viscosity coefficient, the incompressible Navier-Stokes equation is expressed as $\partial_t \boldsymbol{u} + \boldsymbol{u} \cdot \boldsymbol{\nabla} \boldsymbol{u} = -\boldsymbol{\nabla} p + \frac{1}{Re_p} \boldsymbol{\nabla}^2 \boldsymbol{u} + \boldsymbol{f}$, where Re_p is the Reynolds number defined in terms of the constant imposed pressure gradient. Including the pressure gradient in the forcing term, $\boldsymbol{f}$, allows us to assume that both pressure, p, and the velocity field, $\boldsymbol{u}$, are periodic in the streamwise and spanwise directions with respective periodic lengths, L_x and L_z. Including additional artificial terms in $\boldsymbol{f}$ to produce streamwise vortices we have

$$\boldsymbol{f} = -\frac{2}{Re_p}\boldsymbol{e}_x + C_1\{(1-y^2)\cos(k_z z)\boldsymbol{e}_y + \frac{2y}{k_z}\sin(k_z z)\boldsymbol{e}_z\} + C_2\{-y\cos(k_z z)\boldsymbol{e}_y + \frac{1}{k_z}\sin(k_z z)\boldsymbol{e}_z\} ,$$

where $\boldsymbol{e}_i$ denotes the unit vector in the direction of ith space variable, and $k_z = 2\pi/L_z$. Note that solutions obtained in the limit of both C_1 and C_2 vanishing are exact solutions of pure PPF, for which the laminar state is represented as $\boldsymbol{u} = (1-y^2)\boldsymbol{e}_x$.

Henceforth, we assume that the equations have a TWS with streamwise phase velocity, c, and that the solution satisfies two of the three symmetries detailed in the Appendix. We expand unknown variables in Fourier-modified-Chebyshev series satisfying the boundary conditions. Taking into account the imposed symmetries as well as the continuity equation, we can finally deduce from the governing equation quadratic equations for the reduced independent coefficients of the series and c. The quadratic equations are solved numerically by Newton-Raphson (NR) iteration.

3 RESULTS

An initial guess for the NR iteration is provided by a numerical simulation for time-development of the channel flow with $C_2 = 0$ but $C_1 \neq 0$ under the constraints of the symmetries, $\mathcal{A}$ and $\mathcal{B}$. The numerical scheme used is based on that of Ref. 4. If a solution is locally stable for a set of parameters and is close enough to the initial conditions of the simulation in phase space, then the flow field attained eventually by the long-time simulation generally provides a good initial guess for the NR iteration. Fig. 1 shows a projection of a trajectory of the time-development of a trial run. In the projection, an exact TWS is represented as a fixed point, because the solution is steady in a

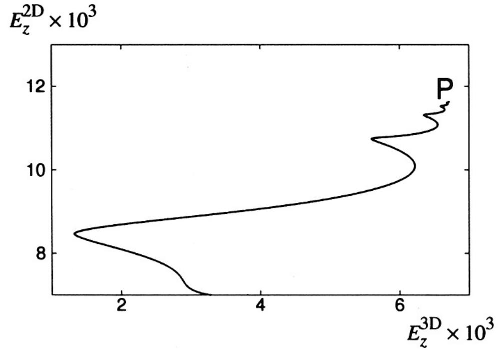

Fig. 1: The trajectory showing the time-development of PPF with a nonzero C_1 calculated by numerical simulation is projected onto the plane spanned by E_z^{2D} and E_z^{3D}, which denote the 2- and 3-dimensional norms of the spanwise component of velocity field, respectively. The point P corresponds to the quasi-stable state that is eventually achieved by prolonged calculation.

frame of reference moving with the phase velocity of the solution on the $x - z$ plane. Adopting the fixed point P shown in the figure as an initial guess for the NR iteration, we obtained two TWSs at $C_2 = C_1 = 0$ by the method of continuation of solutions. These solutions emerge via a saddle-node bifurcation in an Re_p-c projection at around $Re_p \approx 2400$ for $(L_x, L_z) = (\pi, \pi)$.

We additionally searched for another TWS under the constraints of the symmetries $\mathcal{A}$ and $\mathcal{C}$. Performing again the continuation method with the aid of numerical simulation at $C_1 = 0$ but $C_2 \neq 0$, we obtained a further two new solutions converged at $C_1 = C_2 = 0$. From 3-dimensional visualization, as well as the comparisons of the lowest Reynolds number at which these solutions exist, it is, however, concluded that the solutions are the same as the TWSs of PPF obtained previously by Waleffe[15) . Hereafter, for convenience, we refer to these solutions as W solutions, and the upper and lower branches are denoted by WU and WL, respectively.

Streamwise vortices of the present solution can develop across the channel mid-plane, which is illustrated in Fig. 2(a). By contrast, for the vortices of the W solution (Fig. 2(b)), the channel mid-plane can perhaps be regarded as acting like a ceiling, preventing the vortices from spanning the whole channel width. This is because we do not impose a reflection symmetry on the channel mid-plane ($\mathcal{C}$) for the present solutions shown in Fig. 2(a), but such a symmetry is imposed on the W solutions. (The reason why the original W solutions satisfy the reflection symmetry may be readily understood if it is recalled that these solutions were found by homotopy from PCF solutions.) Furthermore, note that a streamwise vortex centered in $y < 0$ is coupled with one centered in $y > 0$, which leads to the formation of large-scale circulations occupying most of the channel width, as seen from the streamlines. For example, the pair of vortices with positive ω_x centered at A and B are involved in a large circulation with positive ω_x spanning the region $0 < z < \pi/2$ and $-1 < y < 1$.

If such a circulation penetrates into the near-wall regions, a correlation between the turbulent fluctuations produced on the upper and lower walls may be a subtle but definite observable in experiments[13)] . On the other hand, the evolution of the circulation in the channel would prevent pure W solutions from realizing in turbulent PPF. In order to qualitatively examine the preference of the PPF, we performed the direct numerical simulation without imposing any symmetry, using as the initial conditions an artificial streaky structure attached on the lower wall with a controlled small 3-dimensional disturbance, "shooting method", introduced in Ref.4. After the flow approached to the TWS, it wandered around on the basin boundary of turbulence for a long time[16,17)] . The flow finally achieved tends to spontaneously satisfy the the symmetry $\mathcal{B}$ rather than $\mathcal{C}$ in the relatively large Reynolds number (Fig. 3 (a)). Note that the near-wall regions are almost laminar and that the LSS is only seen in the center region. This characteristics of the snapshot at high Re is reminiscent of the present solution shown in the Fig. 2(a). As the simulation is performed with the spanwise

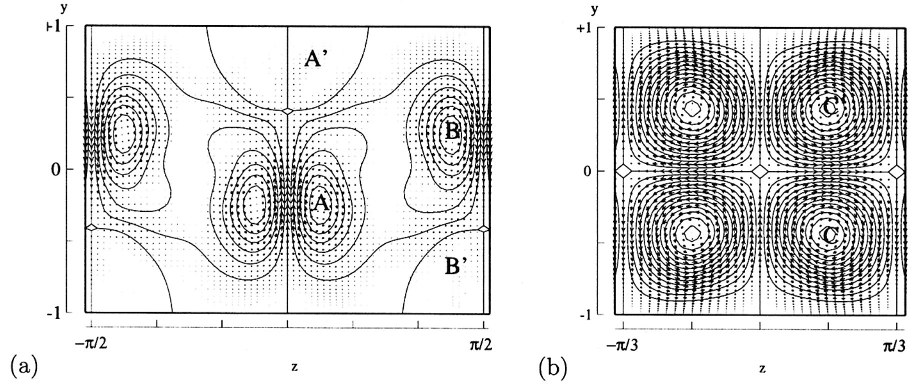

Fig. 2: (a) Streamwise vortices of the present solution for $(Re_{\mathrm{p}}, L_x, L_z) = (2400, \pi, \pi)$ are visualized by vector field of $(w^{2\mathrm{D}}, v^{2\mathrm{D}})$, and its streamlines in the (z, y) plane, where $f^{2\mathrm{D}}(y,z) = \frac{1}{L_x}\int f(x,y,z)\mathrm{d}x$. (b) Same as (a), but for the W solution for $(Re_{\mathrm{p}}, L_x, L_z) = (1006, \pi, \frac{2}{3}\pi)$.

extent $L_z = 0.4\pi$, which is not same as in Fig. 2(a), the accordance would be a casual coincidence. (The dependence of the preferred symmetry of PPF on L_z is the subject of a future study.) However, this fact suggests that the present solution, i.e. its continuations at high Re, might be embedded in fully developed channel turbulence and play a crucial role there if it exists.

4 DISCUSSION

Due to the lift-up mechanism, the large-scale circulations as well as the streamwise vortices promote low-speed streaky regions across the channel mid-plane (Fig. 3 (b)). It may be noted that the wavy modulation shown in the figure bears a similarity to that observed in the W solution with half the spanwise length. Indeed, a further similarity between the W and our solutions can be seen in Fig. 2(a), where the pair of counter-rotating regions still exist on both the walls, for instance, A' against A, or B' against B, as C' against C. Therefore, the mechanism underlying the present solution can be considered to be effectively two SSPs attached to the background shear layers in $y > 0$ and $y < 0$. Note that W solutions of spanwise length $L_z/2$ satisfy symmetry $\mathcal{B}$ as well as $\mathcal{A}$ and $\mathcal{C}$. If a subharmonic perturbation with circulations spanning the whole channel width is added to a W solution with $L_z/2$, it is possible that the present solution may be realized via a bifurcation from the W solution after breaking symmetry $\mathcal{C}$. This suggests that the two SSPs may operate across the channel mid-plane for PPF.

Wang et al.[7] presented numerical evidence that an asymptotic structure of WL in PCF remains in the limit of infinite Reynolds number. This had also been predicted by a truncated dynamical model for SSP, the so called fourth-order model, developed originally to describe turbulent motion in simple shear flows. If we assume that all the x-dependent perturbations are phase-locked and that the non-slip condition is buffered by turbulent fluctuations in the near-wall region, then an analogous simplification may also be applied to the dynamics underlying LSSs in PPF.

Taking into account the symmetries and energy conservation, we will constitute the dynamics by principal modes of the LSS: mean velocity profile (M), streamwise vortices (V), streaky component induced by the vortices (U), x-dependent perturbations (W), large-scale circulations (R), and streaky component induced by the circulations (S);

$$\left(\frac{\mathrm{d}}{\mathrm{d}t} + \frac{\kappa_{\mathrm{M}}^2}{Re}\right) M \;=\; \sigma_{\mathrm{M}} W^2 - \sigma_{\mathrm{U}} UV + \frac{\kappa_{\mathrm{M}}^2}{Re} - \sigma_{\mathrm{R}} RS \;\;,$$

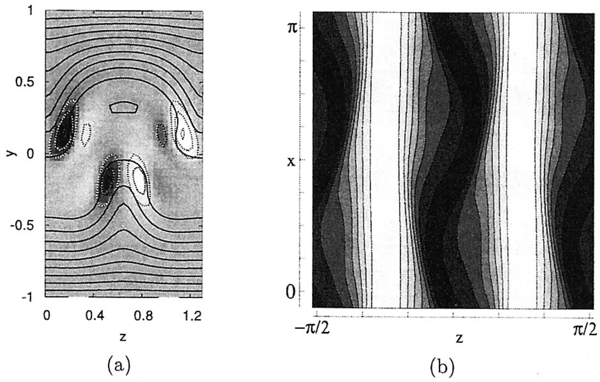

Fig. 3: (a) The cross sectional view of the flow ($Re = 12000$) achieved by the shooting method with imposing no symmetry. The contours for u are from 0 to 1 with increments of 0.1. The grey-level contour levels for ω_x range from -0.3(black) to 0.3(white). (b) The pattern of the low-speed streaky region of the present solution for $(Re_p, L_x, L_z) = (2400, \pi, \pi)$, which is visualized by contours of u at $y = 0$. Contour levels are from 0.66(black) to 0.78(white) with increments of 0.02.

$$\begin{aligned}
\left(\frac{\mathrm{d}}{\mathrm{d}t} + \frac{\kappa_{\mathrm{U}}^2}{Re}\right) U &= -\sigma_{\mathrm{W}} W^2 + \sigma_{\mathrm{U}} M V + \sigma_{\mathrm{S}} R S \ , \\
\left(\frac{\mathrm{d}}{\mathrm{d}t} + \frac{\kappa_{\mathrm{V}}^2}{Re}\right) V &= \sigma_{\mathrm{V}} W^2 \ , \\
\left(\frac{\mathrm{d}}{\mathrm{d}t} + \frac{\kappa_{\mathrm{W}}^2}{Re}\right) W &= (-\sigma_{\mathrm{M}} M + \sigma_{\mathrm{W}} U - \sigma_{\mathrm{V}} V) W \ , \\
\left(\frac{\mathrm{d}}{\mathrm{d}t} + \frac{\kappa_{\mathrm{S}}^2}{Re}\right) S &= -\sigma_{\mathrm{S}} R U + \sigma_{\mathrm{R}} R M \ .
\end{aligned}$$

Following Ref.18, the eigenmodes of the Stokes operator for the modes, M, V, U, R and S, are here determined as $\cos(k_y y)\boldsymbol{e}_x$, $-k_z \sin(2k_y y)\cos(2k_z z)\boldsymbol{e}_y + k_y \cos(2k_y y)\sin(2k_z z)\boldsymbol{e}_z$, $-\cos(k_y y)\cos(2k_z z)\boldsymbol{e}_x$, $k_z \cos(k_y y)\cos(k_z z)\boldsymbol{e}_y + k_y \sin(k_y y)\sin(k_z z)\boldsymbol{e}_z$, and $\sin(2k_y y)\cos(k_z z)\boldsymbol{e}_x$, respectively, where $k_y = \pi/2$. The coefficients in the model, σ_i and κ_i, which are deduced by substituting the sum of the modes into a simplified Navier-Stokes equation, are all supposed to be positive, even for long-wavelength perturbations.

The only extension introduced to the fourth-order model is the additional inclusion of the modes, R and S, which were neglected in the earlier model due to a symmetry in PCF. For PPF, low momentum fluid distributed near both the walls is lifted up towards the channel mid-plane not only by *streamwise vortices attached on the walls* (V) but also by *large-scale circulations* (R), and so two SSPs may interact. The resulting streaky component (U) with wavelength $2k_z$ is observable at the channel mid-plane, while the streaky component (S) with wavelength k_z is observable at one-quarter of the channel height.

Assuming that a steady solution is expressed in a power series of Re, the algebraic system of the equations deduced from the present model possesses four non-trivial steady solutions at least. The two of them, WU and UL, are inherited from the fourth-order model. The other two are nontrivial steady solutions bifurcated from WU and WL via pitchfork bifurcations (here denoted as U and L, respectively). The asymptotic behaviors of U and L are shown in Table 1. These asymptotic behaviors are reminiscent of the LSSs that have been captured as a secondary flow scaled with very long streamwise length at high Reynolds numbers in PPF[11]. Since a governing equation for R is not provided in the present model in order to avoid the difficulty due to introducing another three-dimensional perturbation with the spanwise wavenumber k_z, a degree of freedom, α, remains

Table 1: The asymptotic scaling of principal modes for structures in PCF and PPF are predicted from truncated dynamical models. While L exists only for $0 \leq \alpha$, U does for $-1/4 \leq \alpha$, where $\beta(\alpha) = 2\alpha$ for $-1/4 \leq \alpha < 0$ and $\beta(\alpha) = 0$ for $0 \leq \alpha$. The scaling of WU and WL, which were obtained for PCF, are taken from Ref.18.

	$M-1$	U	V	W	S	R
WU	$O(Re^{-1})$	$O(Re^{-1/2})$	$O(Re^{-1/2})$	$O(Re^{-3/4})$	0	0
WL	$O(1)$	$O(1)$	$O(Re^{-1})$	$O(Re^{-1})$	0	0
U	$O(Re^{-1-\beta(\alpha)})$	$O(Re^{-1/2})$	$O(Re^{-1/2})$	$O(Re^{-3/4})$	$O(Re^{-1/2-\alpha})$	$O(Re^{-1-\alpha})$
L	$O(1)$	$O(1)$	$O(Re^{-1})$	$O(Re^{-1})$	$O(Re^{-\alpha})$	$O(Re^{-1-\alpha})$

unfixed. If we can assume $\alpha = 0$, the mode S ($\lambda_z \sim 2h$) as well as mode U ($\lambda_z \sim h$) may persist as dominant structures in spite of the damping of circulations. This could also be realized in an SSP-like autonomous system closed only by M, R, S and its three-dimensional perturbation with the spanwise length $2h$. The survival of mode S would thus seem to be potentially relevant to the spanwise scale of the LSS reported as $\lambda_z \approx 2h$ in Ref.11 and $\lambda_z = 1.3h \sim 1.7h$ in Ref.12 .

5 SUMMARY

In summary, this study sought to find nonlinear solutions to the Navier-Stokes equations that are relevant to the top of the hierarchy of dynamical systems that characterize turbulent channel flow. In contrast to the previous W solutions, the present solutions possess structures that span the full width of the channel. The direct numerical simulation implied that the LSSs in PPF prefers to the symmetry $\mathcal{B}$ than $\mathcal{C}$. A truncated dynamical model suggested that the present solutions may arise from subharmonic bifurcations from the WU and WL solution branches. The model further predicted the survival of certain asymptotic structures of our solutions in the limit of infinite Reynolds number, with scalings that find tentative agreement with recent DNS results. For PCF, it has been recently reported that WL is stable against spanwise subharmonic perturbations.[7] Possible future studies arising from this work would thus include a detailed analysis of this inconsistency.

6 ACKNOWLEDGEMENTS

This work has been supported in part by KAKENHI (19760123,18540373) and by the Kansai University Special Research Fund, 2009. The numerical calculations were partially carried out on SX8 at YITP in Kyoto University. The authors would like to express their cordial thanks to Dr D. P. Wall for improving the manuscript.

A Symmetry

The symmetries imposed on the solutions are defined by the rule

$$[u_x, u_y, u_z, p]^T(x, y, z) = [u_x, \mu_y u_y, \mu_z u_z, p]^T(x + \nu_x, \mu_y y, \mu_z z + \nu_z) ,$$

where $(\mu_y, \mu_z, \nu_x, \nu_z)$ are constants determined according to the particular symmetry, $\mathcal{A}$, $\mathcal{B}$ or $\mathcal{C}$:

$\mathcal{A}$. Streamwise translation and spanwise reflection, $(\mu_y, \mu_z, \nu_x, \nu_z) = (1, -1, L_x/2, 0)$.

$\mathcal{B}$. Upside-down reflection with spanwise shift, $(\mu_y, \mu_z, \nu_x, \nu_z) = (-1, 1, 0, L_z/2)$.

$\mathcal{C}$. Upside-down reflection, $(\mu_y, \mu_z, \nu_x, \nu_z) = (-1, 1, 0, 0)$.

REFERENCES

[1] S. J. Klines, W.C. Reynolds, F.A.Schraub, and P.W.Runstadler. The structure of turbulent-boundary layers. *J. Fluid Mech.*, **30**, (1967), pp. 741–773.

[2] J. Jeong, F. Hussain, W. Schoppa, and J. Kim. Coherent structures near the wall in a turbulent channel flow. *J. Fluid Mech.*, **332**, (1997), pp. 185–214.

[3] F. Waleffe. Three-dimensional coherent states in plane shear flows. *Phys. Rev. Lett.*, **81**, (1998), pp. 4140–4143.

[4] T. Itano and S. Toh. The dynamics of bursting process in wall turbulence. *J. Phys. Soc. Japan*, **70**, (2001), pp. 703–716.

[5] J. M. Hamilton, J. Kim, and F. Waleffe. Regeneration mechanisms of near-wall turbulence structures. *J. Fluid Mech.*, **287**, (1995), pp. 317–348.

[6] G. Kawahara and S. Kida. Periodic motion embedded in plane Couette turbulence: regeneration cycle and burst. *J. Fluid Mech.*, **449**, (2001), pp. 291–300.

[7] J. Wang, J. Gibson, and F. Waleffe. Lower branch coherent states in shear flows : transition and control. *Phys. Rev. Lett.*, **98**, (2007), pp. 204501–204504.

[8] G. Kawahara. Laminarization of minimal plane Couette flow : Going beyond the basin of attraction of turbulence. *Phys. Fluids*, **17**, (2005), pp. 041702–041705.

[9] H. Wedin and R. R. Kerswell. Exact coherent structures in pipe flow: travelling wave solutions. *J. Fluid Mech.*, **508**, (2004), pp. 333–371.

[10] Y. Miyake, T. Kajishima, and S. Obana. Direct numerical simulation of plane Couette flow at transitional Reynolds number. *JSME Intl J.*, **30**, (1987), pp. 57–65.

[11] J. C. Del Álamo and J. Jiménez. Spectra of the very large anisotropic scales in turbulent channels. *Phys. Fluids*, **15**, (2003), pp. L41–L44.

[12] H. Abe, H. Kawamura, and H. Choi. Very large-scale structures and their effects on the wall shear-stress fluctuations in a turbulent channel flow up to $Re_\tau = 640$. *J. Fluids Eng.*, **126**, (2004), pp. 835–843.

[13] S. Toh and T. Itano. Interaction between a large-scale structure and near-wall structures in channel flow. *J. Fluid Mech.*, **524**, (2005), pp. 249–262.

[14] R. J. Adrian. Hairpin vortex organization in wall turbulence. *Phys. Fluids*, **19**, (2007), pp. 41301(1)–41301(16).

[15] F. Waleffe. Homotopy of exact coherent structures in plane shaer flows. *Phys. Fluids*, **15**, (2003), pp. 1517–1534.

[16] S. Toh and T. Itano. A periodic-like solution in channel flow. *J. Fluid Mech.*, **481**, (2003), pp. 67–76.

[17] A. P. Willis and R. R. Kerswell. Coherent structures in localized and global pipe turbulence. *Phys. Rev. Lett.*, **100**, (2008), pp. 124501–124504.

[18] F. Waleffe. On a self-sustaining process in shear flows. *Phys. Fluids*, **9**, (1997), pp. 883–900.